

FINITE ELEMENT ANALYSIS OF COMPOSITE COLUMNS USING CES DATA

Rohit Kumar¹, Dr. Jyoti Yadav²

¹M. Tech Scholar, Dept. Of Civil Engineering, Sarvepalli Radhakrishnan University, Bhopal, M.P, India.

²Assistant Professor, Dept. Of Civil Engineering, Sarvepalli Radhakrishnan University, Bhopal, M.P, India.

ABSTRACT

New composite structural systems consisting of only steel and concrete, the concrete encased steel (CES) structures, have been developed in Japan to simplify and reduce the cost in construction works for SRC structures. An experimental study on CES column using fiber reinforced concrete (FRC) panel and CES column without concrete cover (CES core column) have been carried out by one of the authors to investigate the seismic performance of the columns. In this paper, a detailed three-dimensional (3D) nonlinear finite element model is developed to study the response and predict the seismic performance of CES composite columns subjected to constant axial and lateral cyclic loads. The columns are modeled using solid elements and analyzed by using finite element program, ANSYS APDL v.14, to investigate the structural performance of the CES columns, which is compared with the experimental results. Numerical results show that CES using FRC panel and CES Core columns had excellent seismic performance with a stable spindle shape hysteresis characteristic and less damage. The presence of FRC panel contributed to flexural capacity about 40% in maximum. In general, the analytical results obtained from the finite element analysis are able to accurately simulate the behaviour of the CES composite columns on the experimental study.

Key words: Concrete Encased Steel, Fiber Reinforced Concrete, Composite Column, Finite Element Analysis, and Seismic Behaviour.

1. INTRODUCTION

Composite steel section and reinforced concrete structure which called SRC structure has been widely used for buildings with more than seven stories in Japan since these structures give an excellent seismic performance with high capacities and deformability. However, some disadvantages of SRC structures are found due to the complexity of construction works, especially in constructing the steel section and reinforced concrete. In order to solve this problem and also to reduce the cost in construction works for SRC structures, concrete encased steel structures consisting of only steel section and concrete, hereafter called to asCES structures, have been developed by Kuramoto in Japan [1]. Figure 1 shows the schematic view and cross-section of CES column.

Some experimental studies have been conducted to examine the structural performance of CES columns [1,2,3]. The results show that the hysteretic characteristics of the CES columns are almost similar to those of SRC columns. The damages of the CES column can be reduced by having the addition of fiber in concrete, known as fiber reinforced concrete (FRC) [2]. The experimental studies on CES columns using FRC panel as a column cover have been conducted by one of the authors in Japan. The CES column is compared to its core (CES Core) in order to know the contribution of the FRC panel on the CES composite column.

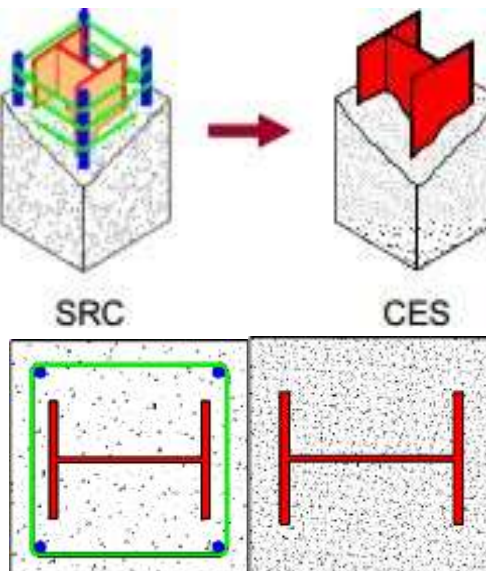


Figure 1 The image and cross section of SRC and CES Columns

In order to validate the experimental results of those composite columns, the three-dimensional finite element (FE) model is developed by using finite element program, ANSYS APDL v.14. A computational model that can be used to perform a structural performance prediction based on a mechanistic analysis has to be developed [4,5]. This paper presents the numerical study on the behavior of CES composite columns, which compared to the experimental data.

2. THE GEOMETRY OF 3D FINITE ELEMENT MODEL

The 3D FE model created for this study replicate the composite column in the experimental program. The software ANSYS APDL v.14 [6] is used to construct the geometry of the model and to view the results (both pre- and post-processing). This software is also used to process the numerical model using the FEM. ANSYS is a commercial FEM package having the capabilities ranging from a simple, linear, static analysis to a complex, nonlinear, transient dynamic analysis [7].

In the FE model, all specimens have a column with 1600 mm height. The column section of CES using FRC panel is 1600 mm², while CES core column is 900 mm². CES column is covered by an FRC panel with a 45 mm thickness, while the core section is the same with CES model. Steel encased in each column has a cross shape section combining two H-section steels of 300 x 150 x 6.5 x 9 mm. Figure 2 illustrates the cross-section and construction of the FE models. The mesh density is chosen so that the element aspect ratio is nearly equal to one.

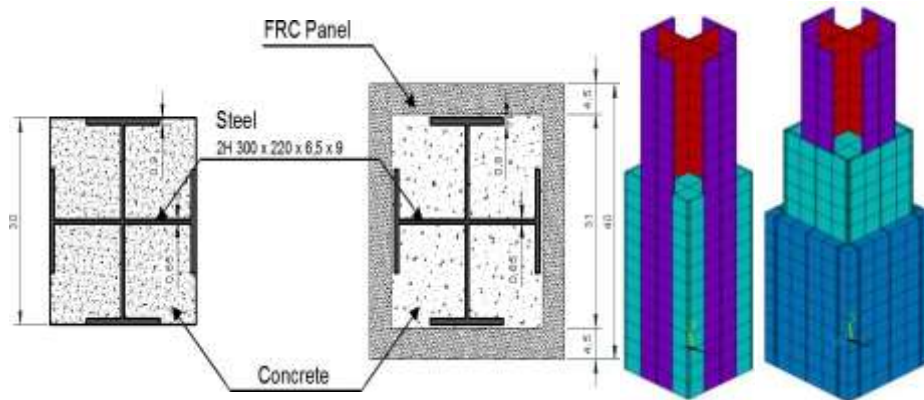


Figure 2 The cross section and construction of FE models

Two types of elements are used in the modeling of steel H-section, concrete, and FRC. ANSYS solid element, SOLID185 is used to model the steel section, while SOLID65 is used to model the concrete [8] and FRC of the columns. The SOLID185 and SOLID65 elements are a 3D hexahedral element defined by eight nodes, as shown in Figure 3.

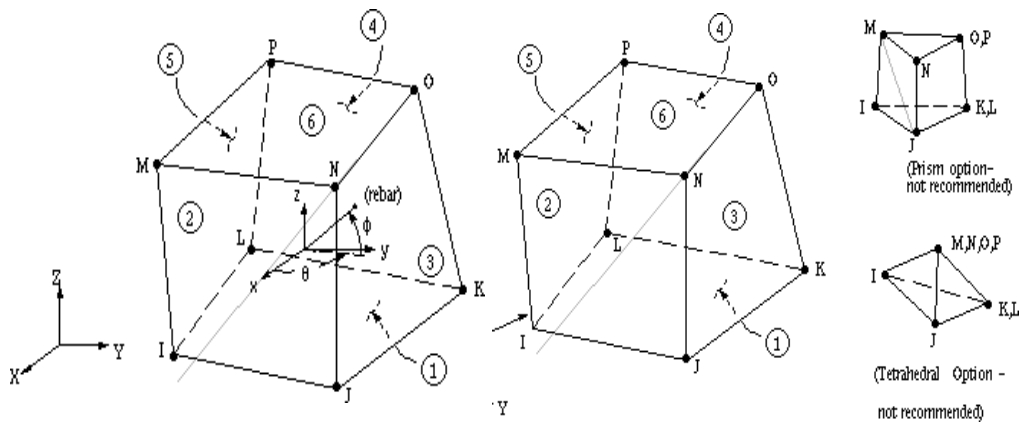


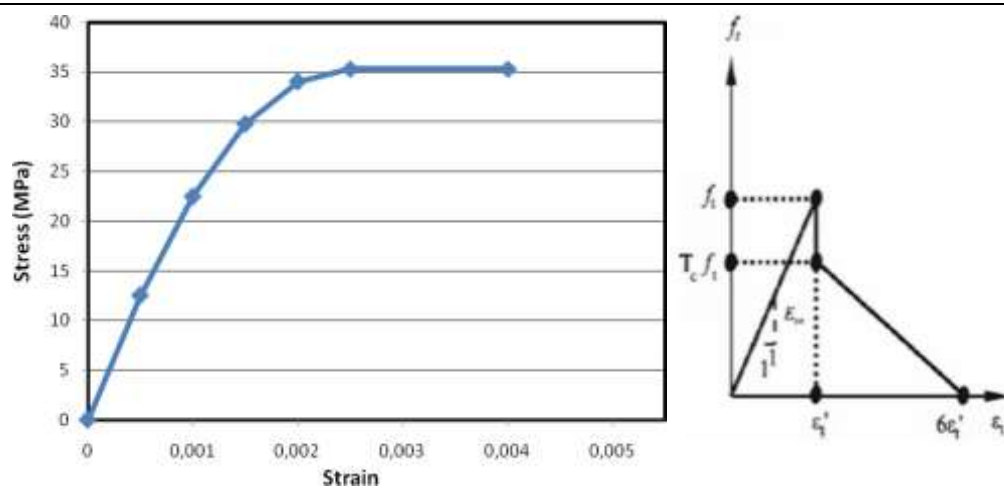
Figure 3 Solid65 and Solid185 ANSYS elements [8]

3. MATERIAL PROPERTIES, BOUNDARY CONDITIONS, AND LOADS

3.1 Materials

3.1.1 Concrete

The compressive strength of normal concrete used in all models is 35 MPa. A peak concrete strain of 0.0025 is used in the analysis, as shown in Figure 4 (a). The stress-strain relationship is designed on the model developed by Saenz [9], which is built into the program. The tensile relaxation (softening) is presented by a sudden reduction of the tensile strength to 0.6 x f_r reach the tensile cracking strain ϵ_{cr} . After this point, the tensile response decreases linearly to zero stress at a strain of 6 x ϵ_{cr} (Figure 4 (b)).



3.1.1.1 (b)

Figure 4 Idealized of compressive (a) and tensile (b) stress-strain curve for concrete [9]

Additional concrete material data, such as the shear transfer coefficient β_t for open cracks and β_c for closed cracks are also needed for the concrete constitutive material data table. A shear transfer developed by Al-Mahaidi [10] is included in the analysis, with a value of 0.75 and 0.9 for β_t and β_c , respectively. The fracture criterion of concrete is applied by the adoption of the five parameter model of William-Warnke [11].

3.1.2 Steel

The yield strength of the steel used in each model is respectively 412.5 MPa and 453 MPa for flange and web steel. The constitutive model of the steel used in this study is a perfectly elastic-plastic criterion. At first, the curve is elastic, then it is assumed to be perfectly plastic (bilinear isotropic model). This curve is suitable for representing stress-strain characteristics of normal and high-quality steel section.

3.1.3 Fiber Reinforced Concrete (FRC)

Mechanical properties of FRC obtained from materials test at the age of 28 days are respectively 39.6 MPa and 7.97 MPa for compressive and tensile strengths. For Specimen CES column using FRC panel, Poly-vinyl Alcohol fiber (PVA fiber: REC100L) with 0.66 mm diameter and 30 mm length is used. The volume content ratios of the fiber are 1.5%. The features and related data of other structural elements in numerical simulations of FRC remain constant and similar to normal concrete.

3.2 Boundary Conditions

The boundary conditions are made to consider of the test setup, as seen in Figure 5. An anchor steel plate/ stub (700.700.400 mm) is used in the model at top and bottom of the column. Nodes at the bottom of the column are restrained in all translational DOF, and top of the column is restrained in the vertical y-direction. The lateral y-direction is restrained since the column prevents any displacement in this direction. The nodes at the two edge lines of the column are coupled in the vertical y-direction to ensure all nodes associated with this line move together, as shown in Figure 6.

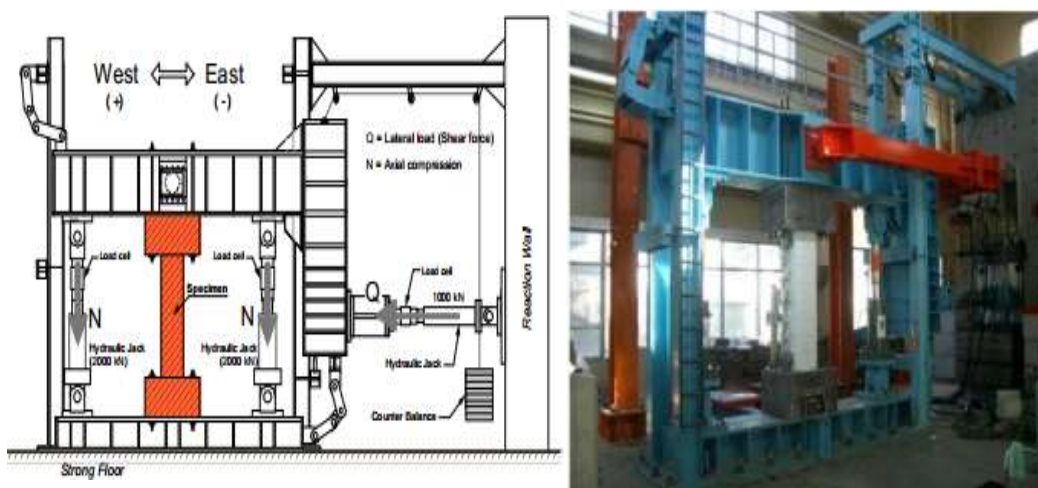


Figure 5 Schematic view and photo of test setup

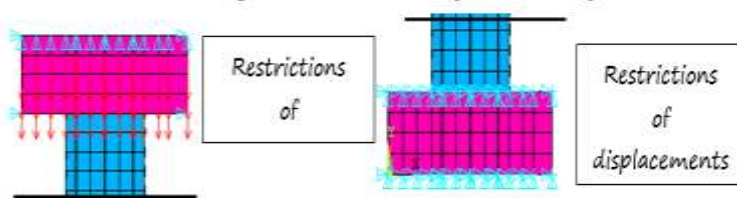


Figure 6 Boundary conditions of FE models

3.3 Loads

The loading in the study is applied as follows: Constant axial load, approximately 770 kN is applied to the top face column for CES composite columns. This is represented in the FE model by applying a point pressure of 1.1 kN on the upper elements (steel plate) of a 717 total nodal area. The lateral loading history for the model is based on story drift and recommended for use in the test program. This is represented in the FE model by applying the displacement in cycles of loading and unloading (load steps) at the top edge of the column. The incremental loading cycles are controlled by story drift, R , defined as the ratio of lateral displacements to the column height, Δ/h . The lateral load sequence consists of one cycle to each story drift, R of 0.5, 1, 1.5, 2, 3 and 4% followed by half cycle to R of 5%, as shown in Figure 7.

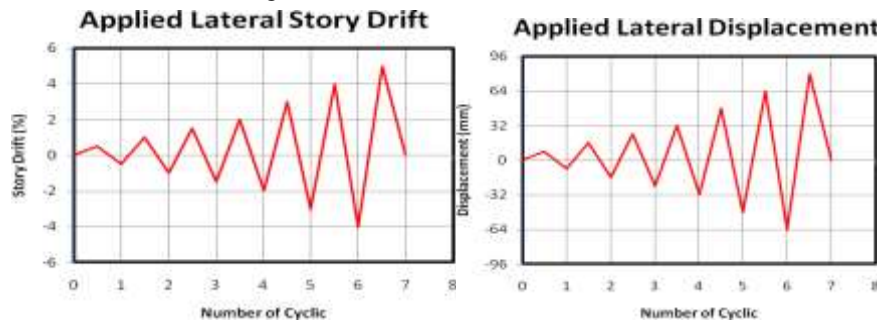


Figure 7 Cyclic lateral load applied in the FE models

The applied cyclic displacements are divided into a series of increments called load steps and load substeps. To predict and control load step size increments, the automatic time

stepping option is turned on in this study. The model stiffness is updated in ANSYS by Newton–Raphson equilibrium iterations. The convergence criteria in this study are based on the displacement of the convergence criteria [12]. ANSYS convergence tolerance default value 5% for displacement checking is initially selected. It is found that convergence is difficult to be achieved using the default values due to the highly nonlinear behavior of the concrete elements and the associated large deflections. Thus, in order to obtain convergence of the equilibrium iterations, the convergence tolerance limit is increased to 10%.

4. RESULTS AND DISCUSSIONS

4.1 Hysteresis Characteristics

The experimental shear force versus story drift (hysteresis loops) for the CES and CES using FRC panel column is compared with those obtained from the FE analysis for the entire loading history, as shown in Figure 8. The analytical results for story shear versus story drift of the FE models show a good agreement with the test results. Both the specimens and models show ductile and stable spindle-shaped hysteresis loops. Table 1 lists the seismic criteria both CES columns and the percentage of its differences between numerical simulation and test results.

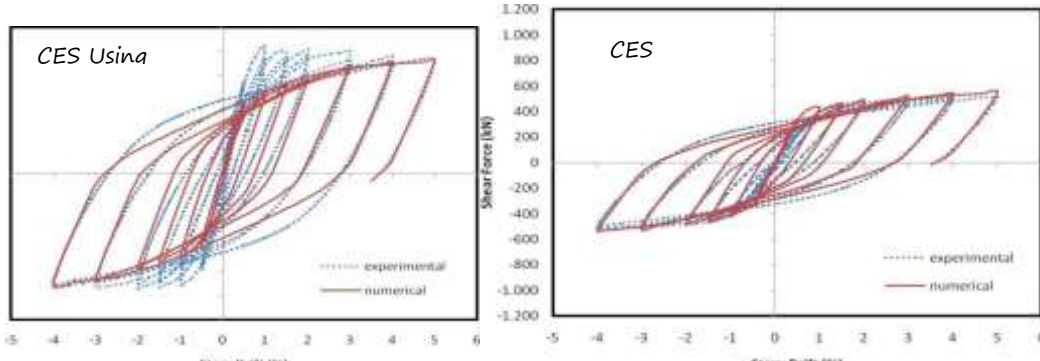


Figure 8 Comparison of hysteresis loops between experimental and numerical results

From the FE model, the maximum lateral shear force for CES column is 541 kN obtained at final story drift 5%. This is approximately 5.2% higher than the results obtained from the experimental (513 kN). It is clear from Figure 8 that the FE and experimental results are almost the same behavior in each stage of cyclic loading. The average of the different percentage of lateral shear force in each stage of loading cycles between the FE analysis and the experimental results is around 5.5%.

The maximum shear force for CES column using FRC panel is 918 kN at R 5% from the FE analysis, which is 12% lower than the experimentally obtained data (1045 kN at R 1%). The FE model behaved lower dissipated energy in the last stages of loading cycles than the experimental data, as seen in Figure 8. The average of the different percentage of lateral shear force in each stage of loading cycles between the FE analysis and the experimental results is around 15%. In the FE model, the peak load in each cyclic always increase, while in the test result, the peak load after R 2% decrease. The difference between the FE and experimental results at different stages of loading can be attributed to mesh refinement, idealized boundary conditions in the FE model, material nonlinearity, and the specified coefficient of friction between contact surfaces at the material interface of the columns. From the FE model, it is found that the presence of FRC panel gives a contribution to flexural capacity by around 40% in maximum, as seen in Table 1.

Table 1 The comparison of seismic criteria of CES Columns between experimental and numerical results

Seismic Criteria	CES Core			CES Core Using FRC		
	Exp.	Num.	Error (%)	Exp.	Num.	Error (%)
Max. Strength (kN)	513	541	5,2	1045	918	12,1
Ductility	5,65	5,88	3,8	6,2	6,3	1,6
Energy Diss. (kJ)	156,4	164	4,9	261	225	13,8
Stiffness (kN/mm)	7,14	7,45	4,3	12,4	12,3	0,8

4.2 Failure Mode and Principal Stress Distribution

The results of FE model show that flexural cracks of CES core appeared at both top and bottom of the column at R 0.5%. Subsequently, the cracks extend at the corners of the column with an increase of the story drift. The crushing of the concrete is observed at the corner of both top and bottom parts of the column and buckling of the steel flange at west side in the bottom part of the column, as shown in Figure 9.

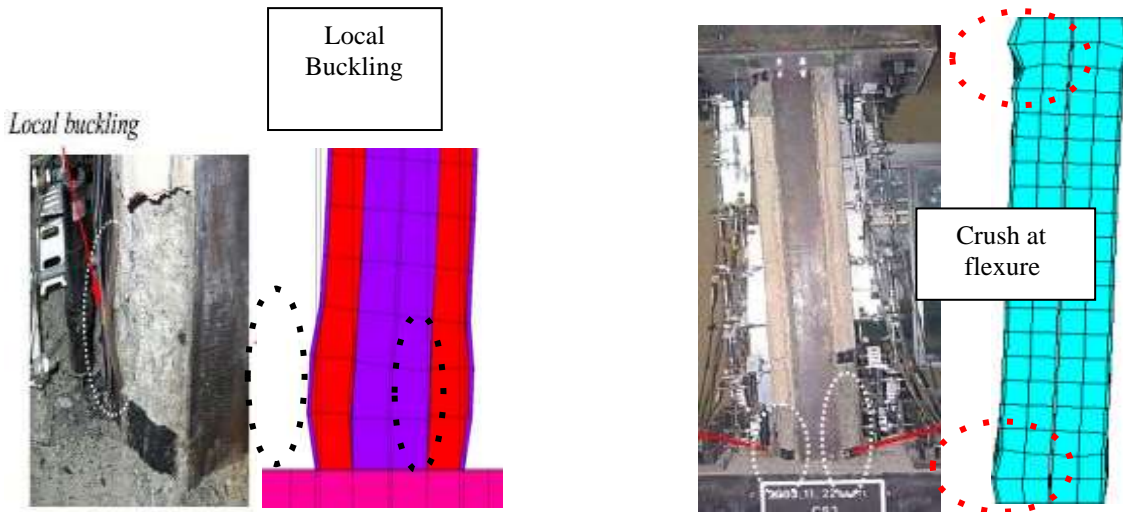


Figure 9 Comparison of concrete and steel in the CES core failure patterns between experimental and numerical results

In CES column using FRC panel model, flexural cracks occur first at R 0.3% at both top and bottom of the column, as shown in Figure 10. With an increase of story drift, the flexural cracks propagate and thin shear cracks disperse all over the column.

The stress and strain in each of material element are also analyzed to validate the FE models. A 0.002 principal strain is respectively reached in the encased steel of CES and CES column using FRC panel models at story drift 0.51% and 1.1%, as indicated that the steel has the first yield in red in Figure 11 (a). These results are almost similar to the test data that the first yield in the corner region both of top and bottom of the steel during experimental are respectively at R 0.88% and 1.1%.

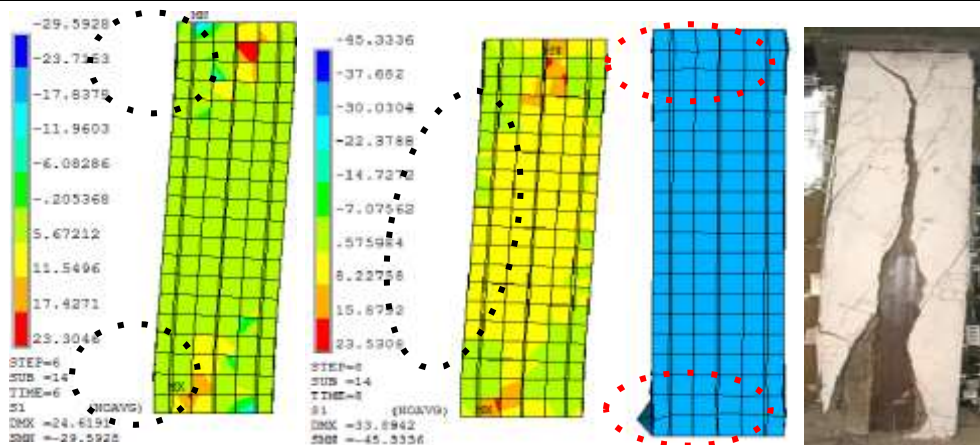


Figure 10 Comparison of FRC panel failure patterns in the CES column using FRC panel between experimental and numerical results

In both CES and CES column using FRC panel models, the first crack in the concrete occurs at R 0.4% in the strut zone of FE model, indicated by maximum principal stresses (tensile) is greater than the tensile strength of concrete (1.8 and 3.1 MPa), as shown inside the oval shape in Figure 11 (b). The cracks occur spread on the strut area and propagate along the horizontal direction. These results indicate that the FE model satisfactorily portray the behaviour of the composite columns.

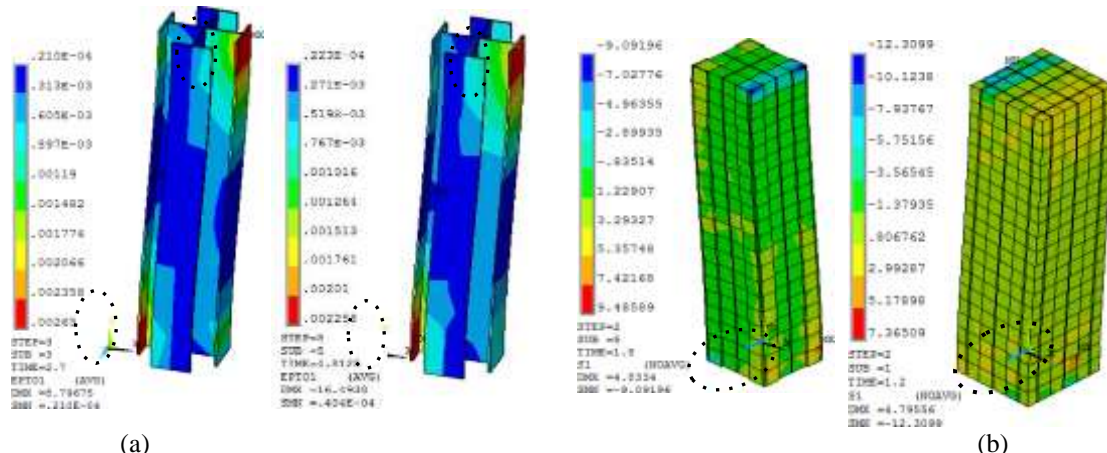


Figure 11 First yield of steel (a) and first crack of concrete (b) in the FE models

5. CONCLUSION

The hysteresis characteristics of the FE analysis correlated fairly well with test results. Good correlation exists in all stages of cycling loading, however, slightly difference of the peak load is observed on CES column using FRC panel on initial loops. The maximum shear force for FE model of CES core and CES using FRC panel are respectively 541 kN and 918 kN

obtained at R 5%. This is approximately 5% and 15% higher than the results obtained from the experimental data. The FRC panel contributes to flexural capacity until large story drift 5%, although the cracks in the FRC appeared after R 0.5%. From the FE model, the presence of FRC panel gives a contribution to flexural capacity about 40% in maximum. The average of the different percentage of lateral shear force in each stage of loading cycles between the FE analysis and the experimental results is around 15%. Generally, the numerical results are able to accurately simulate the behavior of the CES composite columns in the experimental study.

REFERENCES

- [1] Kuramoto, H., Adachi, T., and Kawasaki, K. Behavior of concrete encased steel composite columns using FRC. Proceedings of Workshop on Smart Structural Systems Organized for US-Japan Cooperative Research Programs on Smart Structural Systems (Auto-Adaptive Media) and Urban Earthquake Disaster Mitigation, Tsukuba, Japan, 2002, pp.13-26.
- [2] Adachi, T., Kuramoto, H., Kawasaki, K., and Shibayama, Y. Study on structural performance of composite CES columns using FRC subjected to high axial compression. Proceedings of Japan Concrete Institute, Vol. 25, No. 2, 2003, pp. 289-294.

- [3] Taguchi, T., Nagata, S., Matsui, T., and Kuramoto, H. Structural performance of CES columns using single H-shaped steel. Proceedings of Japan Concrete Institute, Vol. 28, No. 2, 2006, pp.1273-1278.
- [4] Loui, T. R., Satyakumar, M., Padmakumar, R., and Aavani, P. Finite element analysis of coir geotextiles modified flexible pavements based on fatigue failure criterion. International Journal of Advanced Research in Engineering and Technology, Volume 5, Issue 1, January (2014), pp. 112-122.
- [5] Tushal, V., and Skylab, P. B. Finite element analysis of gas turbine rotor with base excitation. International Journal of Mechanical Engineering and Technology, 8(7), 2017, pp. 1362–1369.
- [6] ANSYS Version 14. User's and Theory Reference Manual, 2010.
- [7] Ithikkat, V. V., and Dipu, V. S. Analytical studies on concrete filled steel tubes. International Journal of Civil Engineering and Technology (IJCET), Volume 5, Issue 12, 2014, pp. 99-106.
- [8] John, A., and Usha, S. Analytical study on stress-strain behavior of reinforced concrete column. International Journal of Civil Engineering and Technology (IJCET), Vol. 5, Issue 12, 2014, pp. 45-55.
- [9] Saenz, L. P. Discussion of equation for the stress-strain curve of concrete. Journal American Concrete Institute, 61(9), 1964, pp. 1229–1235.
- [10] Al-Mahaidi, R. S. H. Nonlinear finite element analysis of reinforced concrete deep members, 1979, Rep. No. 79(1), Dept. of Structural Engineering, Cornell Univ., Ithaca, NY.
- [11] William, K. L., and Warnke, E. P. Constitutive model for the triaxial behavior of concrete. Int. Association for Bridge and Structural Engineering, Proc., Vol. 19, 1975, IABSE, Zurich, Switzerland.
- [12] Hawileh, R. A., Rahman, A., Tabatabai, H. Nonlinear finite element analysis and modeling of a precast hybrid beam-column connection subjected to cyclic loads.” J. Applied Mathematical Modelling 34, 2010, pp. 2562-2583.